Contents lists available at ScienceDirect

Chemical Engineering Journal

journal homepage: www.elsevier.com

Online integrated fractionation-hydrolysis of lignocellulosic biomass using sub- and supercritical water

Cristian M. Piqueras [a], Álvaro Cabeza [b], Gianluca Gallina [b], Danilo A. Cantero [b], Juan García-Serna [b, *], María J. Cocero [b]

[a] Planta Piloto de Ingeniería Química, PLAPIQUI-Universidad Nacional del Sur-CONICET, Camino La Carrindanga km 7-CC 717, 8000 Bahía Blanca, Argentina
[b] High Pressure Processes Group, Department of Chemical Engineering and Environmental Technology, University of Valladolid, Escuela de Ingenierías Industriales, 47011 Valladolid, Spain

ARTICLE INFO

Article history:
Received 13 May 2016
Received in revised form 1 September 2016
Accepted 2 September 2016
Available online xxx

Keywords:
Glucose
Glycolaldehyde
Kinetics
Process development
Xylose
Holm oak wood

ABSTRACT

A novel process coupling the fractionation and hydrolysis reactors is presented. Holm oak was used as real lignocellulosic biomass to be treated. In the fractionation reactor, hemicellulose and cellulose were solubilized and partially hydrolyzed in different stages with the aim of feeding the hydrolysis reactor with high C5 concentrations or C6 concentrations. The fractionation was performed in two stages: at 180 °C optimizing the hemicellulose extraction and at 260 °C extracting cellulose and hard hemicellulose remaining in the biomass structure. Three water flows were tested: 11, 17 and 26 cm^3/min. Sugar yields from 71 to 75% were reached, mainly composed of xylose and glucose oligomers and lower amounts of other chemicals, like retro-aldol products, acetic acid or 5-HMF. The outlet stream from the fractionation reactor was directly mixed with sub or supercritical water at the inlet mixer of a SHR where the reaction time was precisely controlled. The temperature, pressure and reaction time were modified to get an insight of their effect on the yield of retro-aldol condensation products. Yields of 24% for glycolaldehyde, and pyruvaldehyde were found at 8.3 s, 350 °C and 162 bar (hydrolysis reactor conditions). On other hand, 25% of lactic acid was found at 0.23 s, 396 °C and 245 bar. A discussion based on a known reaction pathway is proposed. Moreover, a kinetic model for the hydrolysis reactor was put forward, being able to reproduce the experimental data with deviations lower than 10% for sugars and other products extracted. This combined process performs a selective valorization of real lignocellulosic biomass, avoiding the costly process of extreme grinding needed for the fluidization in a continuous hydrothermal process.

Nomenclature

Acronyms

A.A.D.	Average absolute Deviation
Olig	Hemicellulose and cellulose oligomers
C6/OligC5	ratio hexoses to hemicellulose oligomers

Greek letters and symbols

A–G	Parameters for kinetics constant estimation
$\propto_{i,j}$	Stoichiometric coefficient of the compound "j" for the reaction "i", dimensionless
C_{H^+}	Concentration of the protons, mg/L
C_{L_j}	Concentration of the compound "j", mg/L.E_a/R: Activation energy, K
ε	Porosity of the bed, dimensionless
ε_f	Porosity of the bed, calculated at the end of the experiment, dimensionless
ε_{av}	Average porosity of the bed, between the beginning and the end of the experiment, dimensionless
ε_o	Porosity of the bed, calculated at the end of the experiment, dimensionless
K_{L_i}	Kinetic constant, min^{-1}
k	Pre-exponential factor of the kinetic constant, $mg^{-1}{\cdot}min^{-1}$
L	Length of the reactor, m.m_0: initial mass of the solid in the reactor, g
m_f	Final mass of the solid in the reactor, g
m(i) (RM)	Total amount of component (i) in the raw material, extracted by acid hydrolysis and detected by HPLC analysis, g
Mw(i)	Molecular weight of component i, g/mol
MwC	Molecular weight of the carbon atom, g/mol.
$m_{sol}tot(RM)$	Total amount of soluble compounds in the raw material, extracted by acid hydrolysis and detected by HPLC analysis, g
N	Number of compounds, dimensionless
n	Total number of experiments, dimensionless
n(i)	Number of carbon atoms in the soluble component *i*, dimensionless
CKP	Calculated kinetic parameter, activation energy or the natural logarithm of the pre-exponential factor
R^2	Coefficient R^2, dimensionless

* Corresponding author.
Email address: jgserna@iq.uva.es (J. García-Serna)

http://dx.doi.org/10.1016/j.cej.2016.09.007
1385-8947/

r	Ratio between the molecular weight of the soluble compounds extracted and the molecular weight of the atoms of carbon, dimensionless
$r(i)$	Ratio between the molecular weight of the soluble compounds extracted and the molecular weight of the atoms of carbon for compound i, dimensionless
r_j	Reaction rate of the compound "j", mg/min·L
u	Liquid velocity in the reactor, m/min.
t	Residence time in the SHR, s
t_e	Extraction time, min
$t_{e_{\max}}$	Maximum extraction time, min
$x_{i_{EXP}}$	Experimental value of the fitted variable
$x_{i_{SIM}}$	Simulated value of the fitted variable
z	Coordinate along the length of the reactor, dimensionless

1. Introduction

Even if it is reasonably assumed that biomass from plants will be the main carbon source in the future, the choice of which reaction medium should be used to depolymerize and valorize biomass has not been taken yet. Pressurized fluids, especially sub and supercritical water (Tc = 374 °C and Pc = 221 bar), can be pointed as a promising alternative to depolymerize and valorize biomass [1–5]. Physical and chemical properties of water can be modified by adjusting pressure and temperature around the critical point, making water a reaction medium able to favor different kind of reactions [1]. Because of this reason, hot pressurized water has been used as reaction medium for fractionation [6–9], hydrolysis [10–12] and valorization of biomass [13–16].

The composition of lignocellulosic biomass is highly dependent on the plant species and growth conditions. However, it can be considered that the average composition of lignocellulosic biomass is approximately: cellulose (40% wt), hemicellulose (25% wt), lignin (25% wt), extractives and ashes (10% wt) [17]. Although biomass is composed by diverse and complex molecules, it can be fractionated principally into C6 sugars (mainly glucose), C5 sugars (mainly xylose) and lignin [3]. These three fractions can be further modified to produce a wide range of products like: ethanol, hydrogen, glycolaldehyde, pyruvaldehyde, lactic acid and 5-HMF among others [3,18–25].

The fractionation of biomass can be defined as the selective separation of C5 sugars, C6 sugars and lignin from the original biomass matrix. This process was studied under hydrothermal conditions in different ways of operation: batch, semi batch and continuous [3,26]. Semi batch and continuous processes allow obtaining higher yields of sugars and chemical compounds than batch reactors, because it is possible to control the temperature (T) and the residence time (t_r) more accurately than in batch processes [27]. Continuous processes are the most appropriate to control the reaction conditions (T and t_r), however, in most cases it is necessary to apply expensive pretreatments to the raw material before the fractionation + hydrolysis process, for example: exhaustive size reduction [28]. On the other hand, the continuous process can be performed at different operating conditions in order to separate the C5 sugars from the C6 sugars.

The extraction of hemicellulose from woody biomass can be carried out at temperatures between 130 °C and 260 °C, solid reaction times between 20 and 60 min and liquid residence times inside the reactor between 0.1 min and 1 min. At those conditions, hemicellulose can be both extracted and hydrolyzed [29,30]. After the extraction at 180 °C, two products are usually obtained: a liquid composed mainly of C5 sugars and a solid composed of C6 sugars and lignin. These two products can be separated by filtration. Then, the cellulose in the solid can be hydrolyzed at supercritical conditions to obtain a water solution of C6 sugars and a solid enriched in lignin. These processes can be carried out in two reactors with a filtration operation between them. Another option which allows the intensification of the process is using one fixed bed reactor. In such a case, the biomass is loaded in the reactor and the hydrolysis temperature is changed in order to hydrolyze C5 or C6 sugars [31]. The semi batch process allows high performances on the yields of C5 sugars hydrolysis. However, when the reaction temperature is increased to hydrolyze the recalcitrant cellulose and hemicellulose, the yield of recovered sugars decreases because of the increment of the sugars further reactions [10,11,32].

The continuous reactors have been employed in many applications for the valorization of sugar streams allowing a precise control over the reactions [19–21]. These reactions can be managed using pressurized water and choosing the adequate reaction conditions. For example, at temperatures between 200 °C and 300 °C (250 bar) the water molecules are highly dissociated favoring the ionic reactions, like the production of 5-HMF from fructose and glucose [1]. On the other hand, at 400 °C (250 bar) the water molecules are highly associated favoring the non-ionic reactions, like the retro aldol condensation reactions [1].

In this article, a novel integrated fractionation-valorization process was designed and built using wooden biomass as raw material and water (subcritical and supercritical) as reaction medium. The wooden biomass was fractionated in a fixed bed reactor at different temperatures. The solubilized products were directly injected to a continuous near critical water reactor to efficiently convert C5 and C6 sugars into valuable products, like glycolaldehyde, pyruvaldehyde and lactic acid avoiding a further hydrolysis to organic acids. In addition, a kinetic analysis of the biomass hydrolysis was done in order to study the differences in the process when subcritical and supercritical conditions were used.

The objective of this research paper was to design a novel process capable of converting lignocellulosic biomass into valuable products eluding the excessive milling of biomass and decreasing the number of reactors.

2. Experimental

2.1. Materials

Deionized water produced by Elix® Advantage purification system was used as reaction medium to run the experiments. The standards used in a High Performance Liquid Chromatography (HPLC) analysis were: cellobiose (≥98%), glucose (≥99%), xylose (≥99%), galactose (≥99%), mannose (≥99%), arabinose (≥99%), glyceraldehyde (≥95%), glycolaldehyde dimer (≥99%), lactic acid (≥85%), formic acid (≥98%), acetic acid (≥99%), acrylic acid (≥99%), furfural (99%) and 5-hydroxymethylfurfural (≥99%) purchased from Sigma. 0.01 N solution of sulfuric acid (HPLC grade) in Milli-Q® grade water was used as the mobile phase in the HPLC analysis. Sulfuric acid (≥96%) and calcium carbonate (≥99%) supplied by Panreac, Spain, were used as reagents for the quantification procedure of structural carbohydrates and lignin [33]. Also, Milli-Q® water was used in this determination. Holm oak wood employed as raw material was collected in Spanish forests. The wood was milled obtaining chips with average width of 2 mm and average length of 5 mm, as it is shown in Fig. S1 of Supplementary material.

2.2. Analytical methods

The composition of the holm oak wood raw material, exhausted solid and extracted liquor was determined through two Laboratory Analytical Procedures (LAP) from NREL [33,34]. The procedure for solid samples consists in quantifying the structural carbohydrates and lignin in the biomass as follows. A) The biomass was weighted before and after being dried in an air driven oven at 105 °C for 24 h in order to calculate the moisture content. B) Dried biomass was treated in a Soxhlet equipment with n-hexane, leaving a solid free of oils and other extractives. C) 300 mg of dried and free-extractives solid from step (b) were hydrolyzed in 3 ml of 72% wt sulfuric acid solution at 30 °C for 30 min, in order to break the bonds between biopolymers and the main solid structure. D) The mixture of oligomers obtained in step (c) is diluted using 84 ml of deionized water and heated at 120 °C for 60 min with the aim of hydrolyzing hemicellulose and cellulose to obtain their correspondent monomers [35]. E) The solid is separated from the solution by vacuum filtration. F) The total mass of solubilized sugars was quantified as the difference in weight between the original solid and the exhausted solid after oven drying at 105 °C in oven for 24 h. G) The exhausted solid is placed in a muffle at 550 °C for 24 h and the remaining residue was weighted before and after this step to calculate the insoluble lignin and the ash content of the sample. H) A liquid aliquot was analyzed with UV–vis spectrophotometer at 320 nm with extinction coefficient of 34 Lg^{-1} cm^{-1} [36] to calculate the amount of soluble lignin. I) Another liquid aliquot was neutralized to pH range 6–7, then it was filtered using a 0.2 μm membrane and analyzed by HPLC determining the carbohydrates composition. This procedure is performed using a column SUGAR SH-1011 (Shodex) with a 0.01 N of sulfuric acid solution as a mobile phase. To identify the soluble products, two detectors were used: Waters IR detector 2414 (210 nm) and Waters dual λ absorbance detector 2487 (254 nm). In order to calculate the amount of carbohydrates, each chromatogram was integrated numerically by decomposing it into a sum of 9–13 Gaussian peaks, minimizing chi squared function of a Levenberg-Marquardt-Flecher algorithm [37]. Glycolaldehyde and Pyruvaldehyde resulted to be overlapped, since the retention time of their standards is extremely close (11.99 vs 12.24 min, respectively). So we refer to them as glycolaldehyde-pyruvaldehyde.

The raw material contained 1.6% wt extractives, 1.8% wt moisture, 0.2% wt ashes, 24.2% wt Klason lignin (from which 4.0% corresponds to soluble lignin), 45.7% wt of hexoses, 23.9% wt pentoses. The sum of all the components represents the 97.4% of total weight, the discrepancy is due to experimental errors like the loss of solid material after the recovery at the end of the experiments, or the inhomogeneity of the material which can have slightly different compositions depending on the analyzed aliquot; in any case, it is inside the acceptable experimental error.

The amount of C6 was calculated as the sum of glucose, cellobiose and fructose concentrations. Xylose was the only C5 detected. Acetic acid was considered to come from the deacetylation of xylan during the extraction process or, as explained in the next sections, from the hydrolysis of pyruvaldehyde. The hydrolysis products from hexoses and pentoses were mainly glyceraldehyde, glycolaldehyde, pyruvaldehyde, lactic acid, 5-hydroxymethylfurfural and in some cases acrylic acid were detected in very low concentration.

The procedure followed to analyze liquid samples consists in the steps (C), (D) and (I) described above. In this case, the carbon content liquid solutions was determined by total organic carbon (TOC) analysis using a Shimadzu TOC-VCSH equipment. Every sample was previously filtered using a 0.2 μm syringe filter and diluted 1:10 times with Millipore water.

The pH of the outlet stream was measured online using an electronic pH-meter (Nahita model 903).

2.3. Experimental setup and operation procedure

The setup used in this work is shown in Fig. 1. The system consisted of two reactors online integrated: 1) the fractionation reactor (R.1), where the C5 and C6 are solubilized and partially hydrolyzed; 2) the supercritical hydrolysis reactor (SHR), which converts the soluble compounds into added value products. The fractionation line is composed of a water deposit (D.1), downstream an American Lewa EK6 2KN high pressure pump (P.1, maximum flow rate 1.5 kg/h) propels water through a pre-heater (H.1, 200 cm of 1/8″ SS 316 pipe, electrically heated by means of two resistors of 300 W) which ensures an uniform temperature at the reactor inlet. The reactor (R.1), a tube of SS 316, 40 cm length, 1.27 cm O.D., is heated by three flat resistors of 300 W each, placed axially along a machined aluminum bar with 5.08 cm O.D. Both, preheater and the reactor are located in-

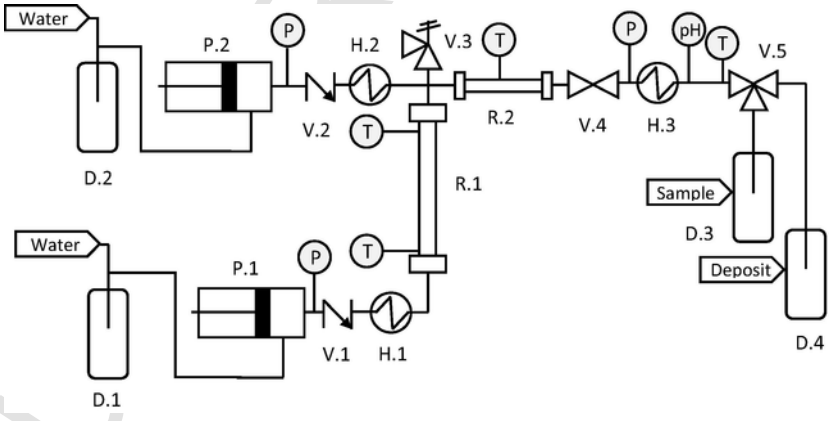

Fig. 1. Experimental setup coupling fractionation and hydrolysis reactors. D.1, D.2: Deionized water deposits. P.1: American Lewa EK6 2KN High pressure piston pump. P.2: Milton Roy XT membrane pump. V.1, V.2: Parker check valve. H.1: Electric low temperature heater, 100 cm of 1/8 in SS316 piping and 2 kW resistor. H.2: 1800 cm of 1/8 in SS316 piping and, high temperature heater and 10 kW resistor. R.1: Fractionation reactor, 40 cm length, ½ in. O.D. SS316 piping. V.2: Parker relief valve. R.2: Second Reactor (SHR) built with ¼ in O.D. SS316 tubing. Two reactors sizes were used 11 cm and 100 cm of length. V.3: Parker relief valve. V.4: high temperature valve Autoclave Engineers 30VRMM4812. IE: 200 cm of concentric tube heat exchanger ½ in.–¼ in. V5: Three way Parker valve. D.3: Falcon® flasks. D.4: 25 L polyethylene products deposit.

side a former chromatographic oven HP5680. The out-flow stream from the extraction line is mixed with the supercritical water stream, entering in a second reactor (SHR) (R.2). The supercritical water line is composed of a heater (H.2), a tube of 18 m, 1/8 in O.D. SS316 wrapped around a brass cylinder and heated by two cartridges and two flat resistors, which provided adjustable power of up to 10 kW, in order to control the temperature of this stream. The water flow was generated by a Milton Roy XT membrane pump (P.2, maximum flow rate 6 kg/h). The SHR allows a fast heating of the biomass stream, which is mixed almost instantaneously with the supercritical water stream, and a rapid cooling of the products, which takes place through a sudden expansion which efficiently stops the hydrolysis. In this way, the reaction time could be precisely calculated, as the reactor works isothermally. Pressure was controlled Micro Metering valve 30VRMM4812 from Autoclave Engineering (V.4). The setups of the two reactors were presented in detail in previous works [32,38].

An average amount of 6.12 ± 0.03 g of holm oak biomass was placed inside the reactor R.1 for each experiment. Two metallic filters were used (pore diameter ≈200 μm), located on the top and bottom of the reactor, avoiding the release of the solid during the experiments. A pressure test with cold pressurized water was carried out before every experiment, with the aim to check the presence of leaks in the system. Then, the supercritical line was heated ensuring the functioning of the system at required operating conditions. Once these conditions were stable, the pumps were switched off and both, the preheater and the reactor R.1, were heated up until the temperatures reached the respective set values. Afterwards, both pumps were switch on again and the flow and pressure were set to the desired conditions, zero time is considered when pressure reached the desired value.

A total of 11 experiments were performed (3 fractionations and 8 coupled reactions), obtaining a total of 130 liquid and 11 solid samples, characterized with the methods described above. Six experiments were performed varying the temperature in the SHR from subcritical (350 °C) up to supercritical (400 °C) conditions, maintaining the pressure at 250 ± 10 bar. The reaction time in this reactor was modified by varying the water flow-rate and changing the reactor volume (2.2 or 12.4 cm^3); reaction times between 0.25 s and to 12 s were tested. Three different water flows (11, 17, 26 cm^3/min) were tested in the fractionation line, maintaining constant the ratio with the flow of supercritical water stream, to get the desired conditions during the further hydrolysis. The feed composition to the SHR was analyzed by carrying out three fractionations without the second hydrolysis stage, at the same conditions of temperatures, flow-rates and pressure tested with the coupled reaction.

The fractionation in the fixed bed reactor was performed in two stages marked by two distinct temperatures: 180 °C to extract the hemicellulose and 260 °C to remove most of the cellulose fraction from the biomass. The heating time between both set points was in the range of 5–10 min, while the flow was temporarily stopped for the experiment running at 26 cm^3/min. In order to follow the reaction evolution, the pH of the outlet stream was measured online sampling every 1 min. Liquid samples (30–40 cm^3) were taken according the pH variations every 5–20 min for the experiment at 11 cm^3/min, and every 2–8 min for the other experiments. The overall experiment time varied from 110, 60 and 45 min for the runs at 11, 17, 26 cm^3/min, respectively (called here as (1), (2) and (3)). After the last sample was grabbed, the heating was turned off and the reactor R.1 was let to cool down to room temperature with air flux. Both pumps were set to zero flow and the system was depressurized. The solid was removed from the reactor, filtered and dried 24 h at 105 °C for further analysis. After cleaning, the fixed bed reactor was placed back, tightened and the system was washed out with deionized water.

3. Results and discussion

3.1. Biomass fractionation

From the analysis of the raw holm oak, the amount of soluble material was 4.65 ± 0.03 g, corresponding to 72.1% of the biomass weight. 3.02 ± 0.02 g of this soluble mass were composed of hexoses (C6) and 1.58 ± 0.01 g of pentoses (C5). The spatial time of the liquid (τ_l), is determined using the liquid flow rate, the reactor volume and the average porosity of the bed (ε_{i0} = 0.457 ± 0.01, ε_f = 0.948 ± 0.019). The latter was calculated by means of Eq. (1), taking into account the initial and the final fraction of void volume in the bed, due to the shrinking size of the biomass particles, and also considering a constant density for water [38] (since its variation with temperature is less than 2%) and a constant density of the holm oak wood (800 kg/m^3, dry based for holm oak species). In this sense, residence time for the liquid inside the fixed-bed reactor was in the range of 1.0 min < τ_l < 2.1 min.

$$\varepsilon_f = \varepsilon_0 + (1 - \varepsilon_0)\frac{(m_0 - m_f)}{m_0} \tag{1}$$

Fig. 2 shows the cumulated mass of total soluble materials, oligomers and monomers of C5 and C6, as well as products deriving from the further reaction of sugars. These values were determined using TOC and HPLC analysis of the products. The different conditions were obtained by changing water flow-rates in the fractionation line for the experiments 1, 2 and 3. The dashed lines signals the time when transition between the two temperature stages takes place. The mass of soluble compounds detected by TOC was calculated by dividing the value of total organic carbon concentration recognized by the equipment by a factor 0.42 (Eq. (2)).

$$r = \sum_1^c r(i) = \sum_1^c \left(\frac{m(i)}{\sum_1^c m(i)}\right)\left(\frac{n(i)MwC}{Mw(i)}\right) = 0.42; \qquad i = 1. \tag{2}$$

The factor *r* is the sum of the ratio between the molecular weight of carbon atoms in the soluble compounds extracted from raw material to the molecular weight of the compounds itself. This value is an approximation that allows comparing the mass obtained by TOC analysis (total amount of C) with the mass quantified by HPLC (total amount of soluble compounds).

This approximation is based only on the sugar contents and it is used as a general value for all the experiments. It does not consider the effect in the carbon ratio of the condensation and dehydration reactions happening during the extraction and hydrolysis. In addition, it does not take into account the amount of soluble lignin since it is relatively low (only a 4% in the raw material, see Section 2.2). However, in all the experiments, the mass balance matched with a maximum error around 20%.

The overall material balance was calculated by summing the mass of the solid recovered from the reactor R.1 at the end of the experiment to the mass of the soluble material estimated using the quantified amount by TOC and the assumed factor showed in Eq. (2); and the mass of insoluble lignin flushed by the water stream. For experi-

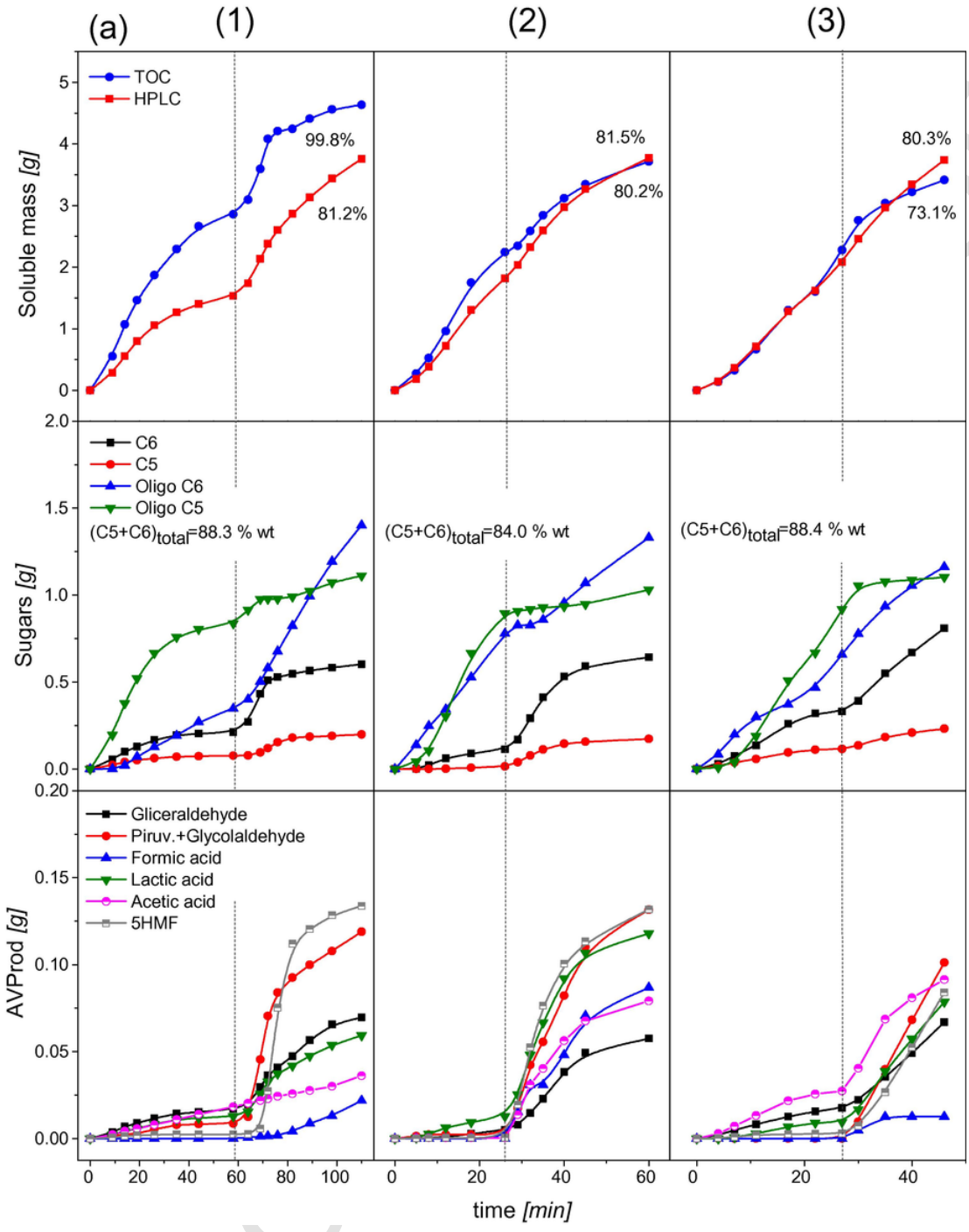

Fig. 2. Product distribution and mass balance in the biomass valorization. (a) Results from the fractionation without further hydrolysis for 11, 17 and 26 cm^3/min in the extraction line. The first line of graphs represents to the percentage of soluble compounds identified by total organic carbon (TOC) and HPLC. The yields, calculated by the obtained soluble fractions [g]/(4.65 g), are showed above each curve. Second row of graphs in Fig. 2 shows the amount of carbohydrates in the form of sugars and oligomers. The last row displays the time evolution of the products derived from the hydrolysis of sugars in the fixed bed reactor. (b) Products distribution at 380 °C. (c) Product distribution at 350 °C. (d) Product distribution at 400 °C and short residence times. In experiment 11, the absence of water flux in Reactor 1 makes heating process it faster (5 min). We choose this option in order to avoid a large transition state.

ments 1, 2 and 3, this mass balance was equal to 103.8, 93.7 and 84.9% related to the amount of biomass fed to the reactor.

The mass of soluble material obtained by TOC with the same values obtained by HPLC for each sample are compared in the first row of graphs in Fig. 2 (a). The values plotted in Fig. 2 are the yields of soluble compounds obtained from each technique related to the same amount in the raw biomass (calculated as observed soluble compounds [g]/4.65 g). The discrepancy between both values is reduced when the water flow-rate through the extraction reactor is increased from 11 to 26 cm^3/min (23.6, −4.1 and −3.2% for the three flows, respectively). This fact could be explained by the increasing production of compounds derived from the sugars hydrolysis (mainly organic

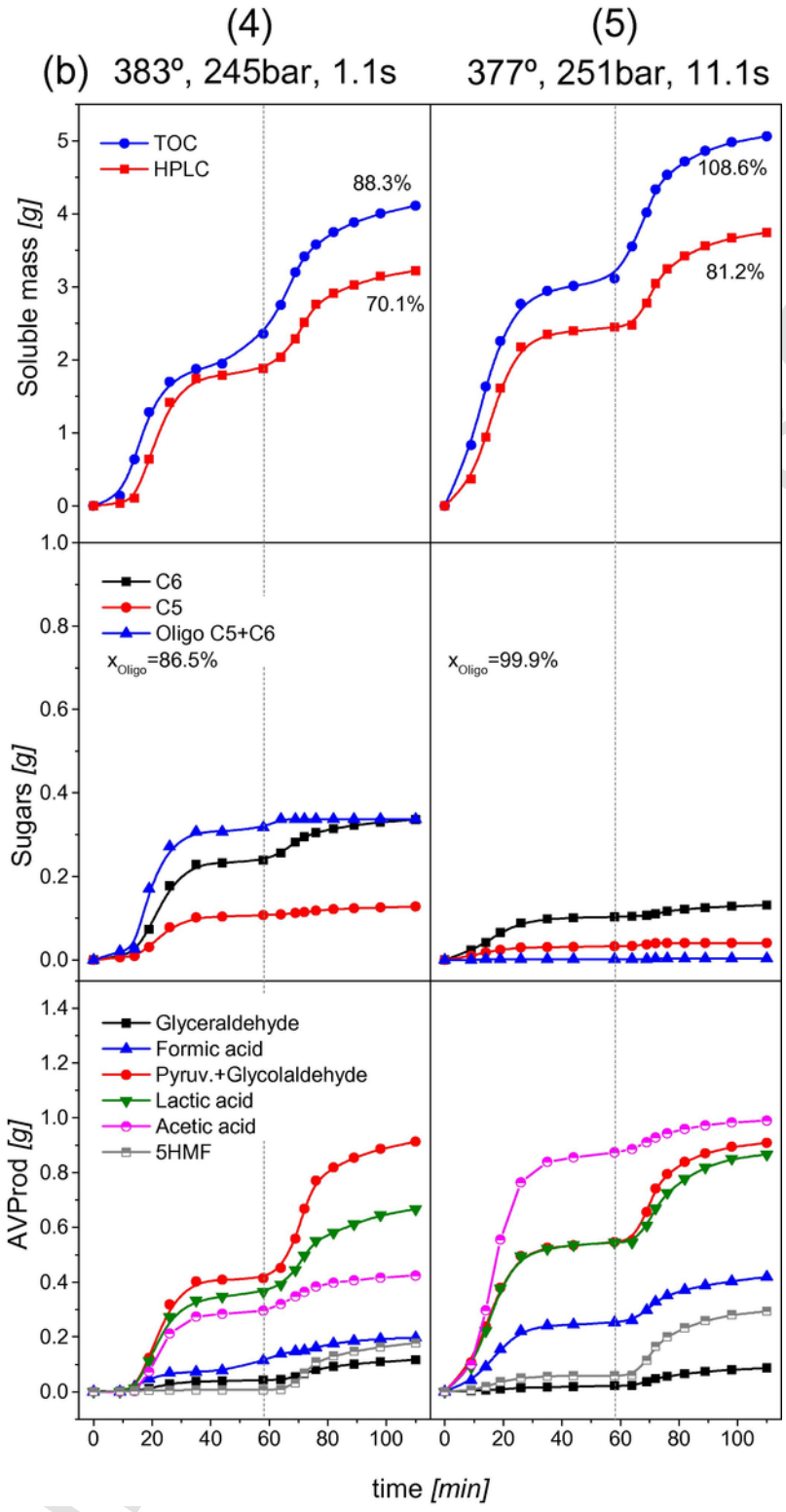

Fig. 2. (*Continued*)

acids) not identified by HPLC or whose value is so low that it cannot be detected. From HPLC chromatographs of experiment 1, some peaks do not fit with the retention time of the 17 standard compounds identified in this column (e.g. Fig. S2 in Supplementary material). Besides, some other peaks were not completely resolved. The amount of sugars and soluble oligomers of C5 and C6 obtained from fractionation are displayed in the second line of graphics in Fig. 2 (a). Most of the hemicellulose is hydrolyzed to oligomers, in fact hemicellulose is highly soluble in water because of the abundance of acetyl groups

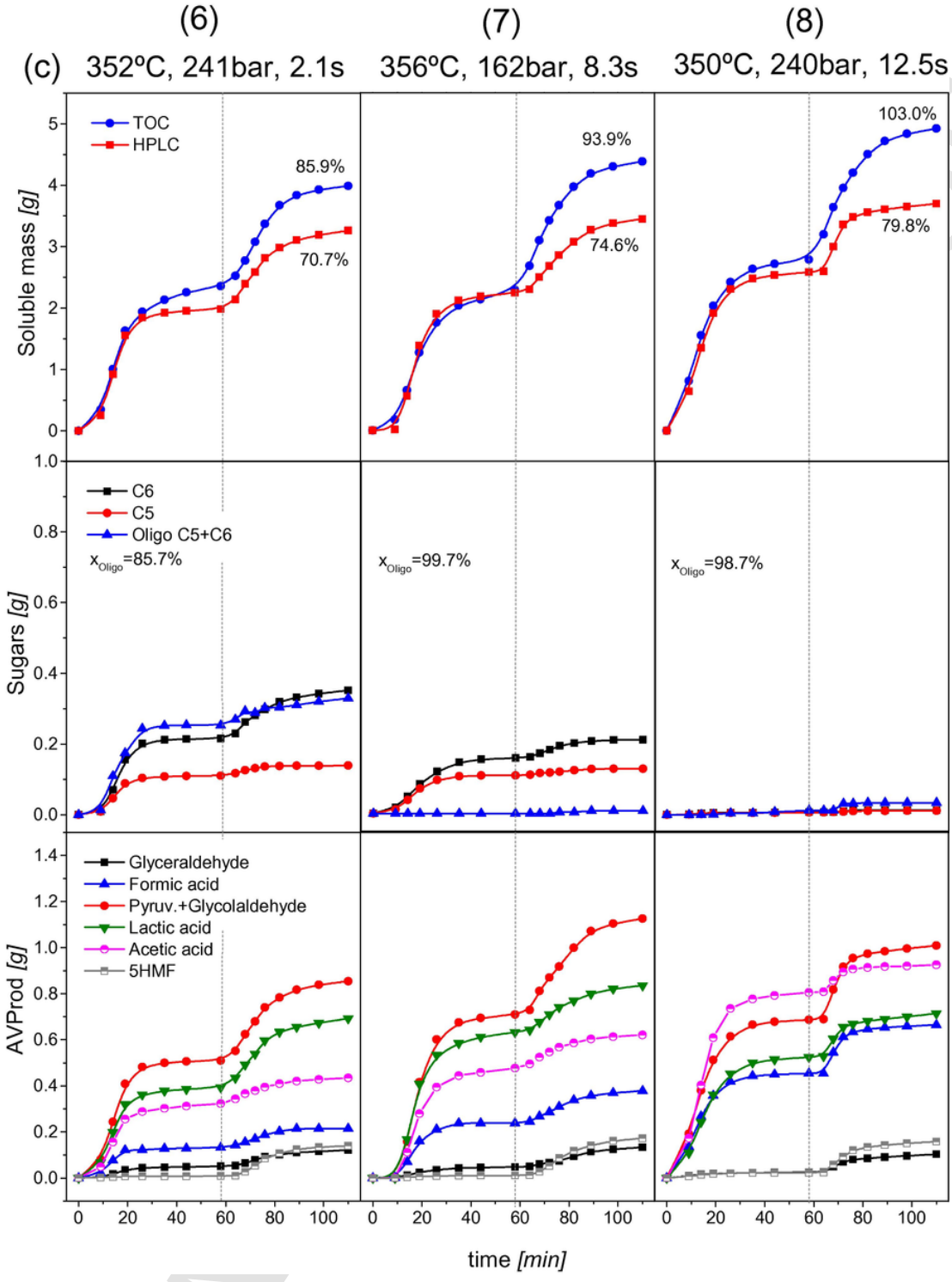

Fig. 2. (*Continued*)

in its amorphous structure [39], and after the first breaking leads to the production of soluble oligomers.

The yield of C5 at the end of second stage of temperature was 87.3, 89.8 and 93.1%, for experiments 1, 2 and 3, respectively. On the contrary, the crystalline nature confers to cellulose a water insoluble character, so, the oligomers with only very low molecular weight would be water soluble [40]. In this sense, when the flow rate increases in R.1 (decreasing τ_1), cellulose is hydrolyzed mainly to hexoses in oligomer form, giving rise to lower amounts of monomers. This result is observed by comparing the amounts of C6 oligomers (Oligo C6) to monomers (C6) in experiment 1 respect to experiments 2 and 3. This selectivity to oligomers occurs mostly during the first stage of temperature in R.1 (see second row of graphs in Fig. 2 a). The oligomers quantification was obtained from the difference be-

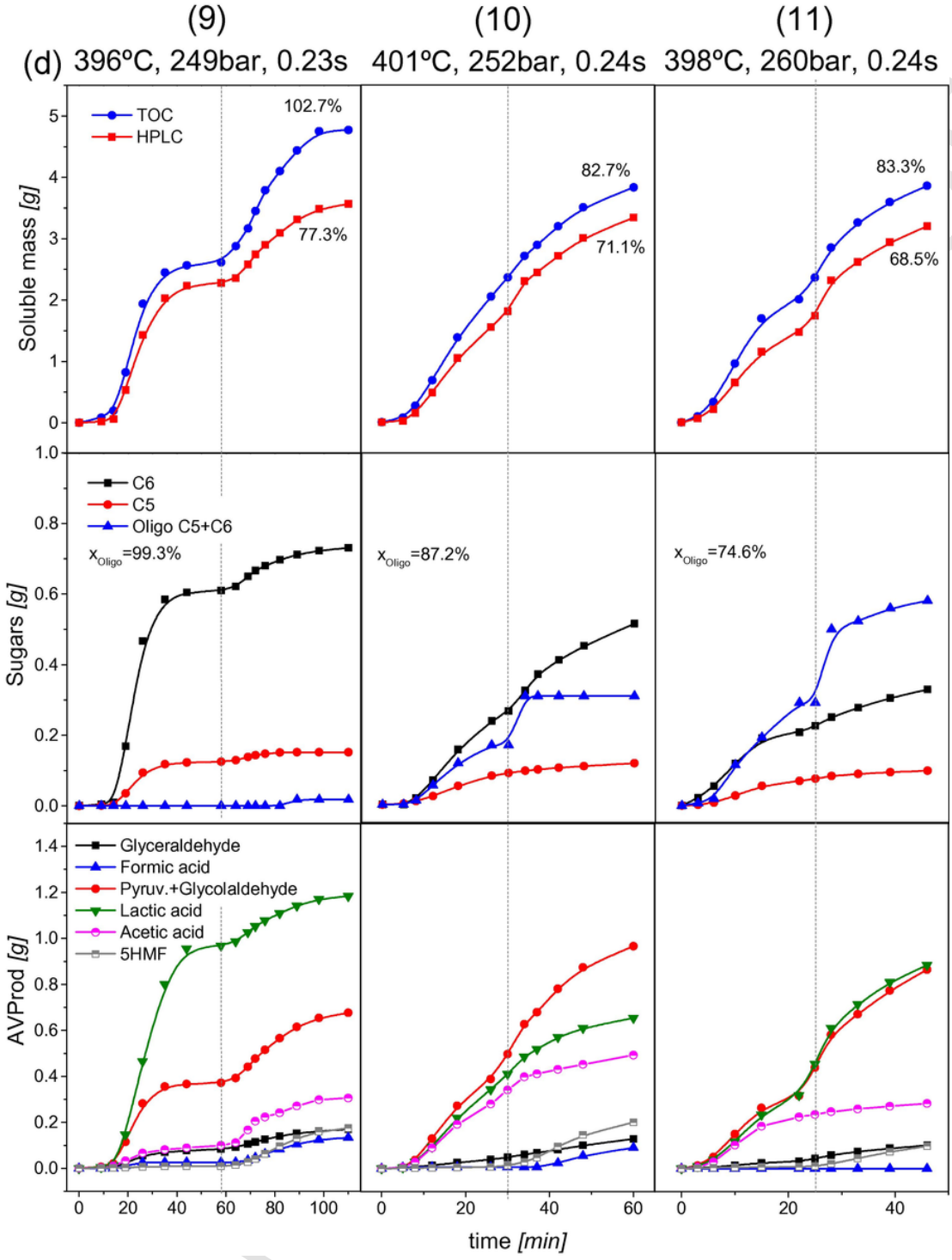

Fig. 2. (*Continued*)

tween glucose, cellobiose, fructose and xylose of the liquid containing all the soluble sugars and the same compounds obtained from the total acid hydrolysis of this liquid [38]. So, high liquid spatial times enhanced the hydrolysis and solubilization of hexoses. This distribution could be related to the difference in the activation energy of the cleavage of the hydrogen bonds between celluloses and the α1-4 glycosidic bond hydrolysis, which is known that is favored at subcritical conditions [10,32]. The last row of graphs in Fig. 2 (a) displays different amounts of products from the hydrolysis of xylose, glucose and fructose. These amounts are depreciable at the first stage and are increased after temperature is raised. However, these compounds are one order of magnitude lower than the soluble sugars during the extraction. An example is 5-HMF, which is produced mainly in the second stage of fractionation temperature where the conditions make the water a highly ionic medium in the reactor R.1. The main components in the output stream were pyruvaldehyde, glycolaldehyde and

lactic acid. The decrease of the reaction time of liquid inside the reactor diminished the further transformation of sugars.

3.2. Biomass valorization with sub and supercritical water hydrolysis

The outlet stream from the fixed bed reactor was fed to the SHR together with a water stream at temperatures and pressures above to its critical point. The aim was to obtain a fast and selective hydrolysis of the oligomers and sugars extracted from the biomass. The reaction time in the supercritical reactor (*t*) was varied in order to modify the selectivity to different chemicals.

The optimum temperatures and flow-rates in R.1 have been identified in extraction step, as they lead to the maximum yield of soluble material. For this reason, a flow rate of 11 cm^3/s and temperatures of 180° and 260 °C (for the two stages, respectively) were chosen for most of the experiments. Only the experiments 10 and 11 were performed with the same liquid flow-rates used in the fractionation experiments 2 and 3 (17 and 26 cm^3/s, respectively).

This approach also allows knowing the composition of the stream entering in the second reactor. Eight experiments were performed, as shown in Table 1. Three temperatures and 6 reaction times were tested, keeping constant the temperatures of water through the first reactor.

Three reactions (5, 7 and 8) were performed in a longer reactor (100 cm), aiming to increase the residence time in SRH (*t)*. A lower pressure was used in reaction 6 (162 bar) to observe the influence of water density in the products distribution.

Overall mass balance for each experiment, calculated as described in ection 3.1, is presented Table 1. Mass balances indicate that no significant gasification takes place in the supercritical reactor. First row of graphs in Fig. 2 (b), (c) and (d) presents the mass of the soluble materials quantified in the outlet stream of SHR by TOC and HPLC. The percentage yield of each experiment respect to the soluble mass in the raw holm oak is presented as the number in the each graph. Some differences between these two procedures are observable, mainly increasing t_e in the second stage of fractionation or at higher sugars conversion. These findings could be related to the production of small organic acids, ketones and aldehydes (levulinic and acrylic acids, dihydroxyacetone, formaldehyde) and other compounds not identified by HPLC, see Fig. S2 in Supplementary material. This hypothesis agree with the decrease of the mass difference observed by both techniques when a high water flow is involved (as commented in Section 3.1), indicating an over breaking and oxidation of the products of interest at higher *t*.

3.2.1. Oligomers and sugars conversion

Oligomer conversion to C5 and C6 monomers was calculated by difference between the stream entering to the SHR (composition obtained in experiment 1 corresponding to reactions 4–9 and composition of experiment 2 and 3 for experiments 10 and 11, respectively), and the stream leaving the reactor after the hydrolysis.

The conversion of oligomers to C5 and C6 monomers are reported in the seventh column of Table 1. In all the runs, oligomers conversion was higher than 85%. The exception was experiment 11, in which the small *t* and high dilution (four times lower than in the experiments 4–8) could be the cause of the low conversion. C5 Sugars (xylose) and C6 (cellobiose, glucose and fructose) are intermediate compounds in the reaction pathway. Conversion of sugars is faster than cleavage of oligomers to monomers at subcritical temperatures and even at a temperature a little higher than the critical point of water (e.g. 380 °C). This is showed by comparing the amount of Oligo C6 and Oligo C5 with C6 and C5 in experiments 4 and 6 (see Fig. 2 (b) and (c)). A different behavior is detected near to 400 °C, like in experiment 9, where oligomers conversion seems to be faster than sugars hydrolysis, in agreement with the observations reported in the literature for oligomers originating from microcrystalline cellulose [5][11]. Surprisingly the time needed for a complete conversion of sugars is quite larger than the pure cellulose hydrolysis at the same temperature (eg. 350 °C: 2 s in Ref. [29] vs 12 s in this work). This could be related to the hydrolysis of C5 and C6 contained inside the porous structure of fluidized microparticles of biomass coming from the reactor R.1 with the stream of fluidized biomass. Also the presence of other ions or compounds could be linked to this attenuation.

3.2.2. Added value products (AVP) from the sugars hydrolysis

The third row of graphs in Fig. 2 (b), (c) and (d) displays the amount of added value chemicals (AVP) (glyceraldehyde, glycolaldehyde, pyruvaldehyde, lactic acid, formic acid, acetic acid and 5-HMF) produced from hydrolysis of cellobiose, glucose, fructose and xylose. The reaction pathway of cellulose hydrolysis involving oligomers and cellobiose as intermediaries was reported in the literature [32]. Xylose hydrolysis in near critical and supercritical water

Table 1
Temperatures, pressures, residence times, mass balance and oligomers conversions of the experiments coupling Fractionation + Hydrolysis reactors.

Exp	T [°C]	P [bar]	t^1 [s]	$Q_{SHR}{}^2$ [cm^3/min]	$MB_{TOC}{}^3$ [%]	$x_{Oligomers}{}^4$ [%]	$Y1_{AVP}{}^5$ –	$Y2_{AVP}{}^6$ –
4	383.7 ± 5.1	245.7 ± 4.6	1.06	36.0	92.2	86.5	0.008	0.079
5	377.2 ± 3.5	251.9 ± 5.9	11.15	38.5	105.9	99.9	0.247	0.281
6	352.5 ± 4.4	241.3 ± 3.7	2.10	35.2	89.3	85.7	0.004	0.109
8	349.9 ± 2.4	239.6 ± 4.2	12.50	35.8	103.1	98.7	0.233	0.132
9	396.1 ± 3.6	249.1 ± 5.1	0.23	36.8	103.6	99.3	0.440	0.254
10	401.2 ± 2.8	252.2 ± 3.9	0.24	90.1	93.0	87.2	0.481	0.278
11	398.3 ± 3.0	259.9 ± 3.4	0.24	106.2	91.2	74.6	0.530	0.228

[a] Residence times were calculated based on the concepts drawn in reference [32].
[b] Mass balance accounts the amount of solid recovered from the Extraction reactor adding the mass of insoluble lignin flushed in the water stream and the total mass solubilized measured by TOC.
[c] Oligomers conversion involves the mass of oligomers quantified by HPLC outcoming from the Fractionation related to the mass of oligomers in the outlet stream of the sub-supercritical reactor.

1 t: reaction time in hydrolysis reactor.

2 Flow rate in the SHR.

3 Global mass balance of the coupled process.

4 Conversion of oligomers from hemicellulose and cellulose.

5,6 Yields of added value products in the time period of the first and second stage of temperature during fractionation Y_i = $mass_i$/mass soluble material in raw biomass.

was analyzed by several authors [41,42]. The combined pathway is presented in Fig. 3. Not all the products involved in this scheme were identified by the liquid chromatography. The cellulose and hemicellulose pathways are similar. They involve two consecutive hydrolysis steps, the first one in which the oligosaccharides are hydrolyzed to glucose and xylose, respectively, and the second one in which glucose and xylose are implicated in two possible routes: isomerization and dehydration or retro-aldol condensation [18,42]. Glucose can follow a reversible isomerization to produce fructose, however, the reverse reaction is almost inhibited at the same conditions [19,20]. Glucose can also be transformed into 1,6 anhydroglucose and fructose can be transformed into 5-hydroxymethylfurfural through a dehydration reaction [43]. The other alternative of glucose conversion is the retro-aldol condensation producing glycolaldehyde and erythrose [32,44]. Erythrose is further transformed into glycolaldehyde by the same reaction mechanism [18]. The retro-aldol condensation reaction of fructose produces glyceraldehyde and dihydroxyacetone. These molecules are further isomerized into pyruvaldehyde [19], which is transformed to lactic acid by an extra oxidation. Hemicellulose hydrolysis is quite similar; the first step is the depolymerization to produce xylose and xylose oligomers. After that, xylose can be isomerized to D-xylulose, assuming that D-xylulose as an intermediate for furfural and retro-aldol products (glyceraldehyde, pyruvaldehyde, glycolaldehyde, lactic acid, dihydroxyacetone, formaldehyde) [41,42]. This reaction pathway consists of a retro-aldol reaction (Lobry de Bruyn-Alberta van Ekenstein (LBET)) from D-xylose and D-xylulose, similar to that involving D-glucose and fructose.

In the experiments, a considerable amount of glycolaldehyde-pyruvaldehyde and lactic acid was observed. The distribution of these chemicals was similar for experiments 4 and 6 (Fig. 2 (b) and (c)) in spite of the difference of water properties at both temperatures. At 352 °C and 241.3 bars, the water density and pKw are 614.7 kg/m^3 and 11.7, respectively. On the other hand, at 383 °C and 245.7 bar, those properties take a value of 319.7 kg/m^3 and 15.3, both calculated as developed in literature [1]. A little difference in the amount of glycolaldehyde-pyruvaldehyde as well as in the 5-HMF is perceived, principally at times corresponding to the first stage of temperature of the reactor R.1. This means that this variations of density and Kw, do not modified largely the selectivity between isomerization-dehydration and retro-aldol pathways like it does in the pure cellulose hydrolysis. In this last, isomerization of glucose to fructose is highly inhibited by decreasing density [32]. This behavior could be explained by the presence of H^+ ions coming from the deacetylation taking place during the fractionation, in addition to the H^+ produced by the water ionization. Also, considering the nature of raw biomass, other ions in solution could be present. Under 352 °C and pressure, isomerization of glucose to fructose and further dehydration is favored for pure cellulose hydrolysis [43]. But, in the present cases, the high yields of glycolaldehyde-pyruvaldehyde and lactic acid are evidences that the retro-aldol pathways take place as well. Experiments 4 and 5 were performed at similar temperature and pressure but involving different residence times (t = 1.06 vs 11.15 s, respectively). For experiment 5, the acetic acid amount was highly increased, mostly in the time period corresponding to the first stage of temperature in R.1. This acetic

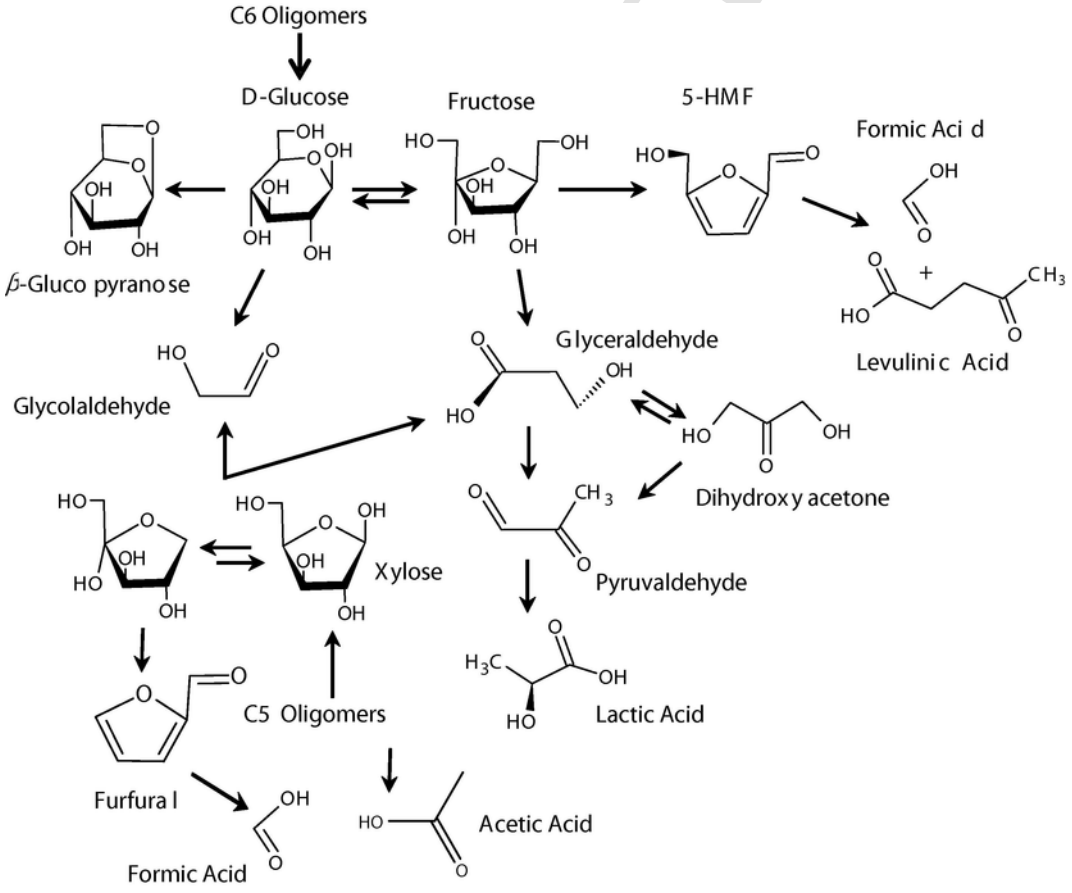

Fig. 3. Combined reaction pathway of oligomers C5 and C6 including the glucose and xylose further reactions in hot pressurized water.

acid exceeded the amount produced in the hemicellulose deacetylation. Besides, acetic acid could be obtained directly from lactic acid decarbonylation [15]. Both, glucose and xylose, are able to produce lactic acid by means of the retro-aldol pathway with glyceraldehyde and pyruvaldehyde as intermediaries (see Fig. 3). In this sense, these retro-aldol pathways could explain the extra amount of acetic acid obtained at longer residence times in the SHR. Fig. 4, displays the pH of the output stream after the fractionation stage (experiment 1) and the coupled process fractionation + hydrolysis (experiments 4, 5, 6 and 8). The pH in the outlet stream, after SHR, was always lower to the pH of the output stream from the fractionation step itself. This observation agrees with the fact that extra amount of acetic acid was produced when a deeper hydrolysis was performed (see experiments 5 and 8). After this, no difference in the pH can be detected. Similar behavior was observed from experiments 6 and 8, in spite of the difference of formic acid produced in both (see Fig. 2 (c)).

The pressure change in the range studied, had no effect on the chemicals distribution (see Fig. 2 (c), experiments 6 and 7). Under the conditions of experiment 7, pKw is 11.9, calculated by means of an empiric equation [45]. This value is quite similar than pKw of the experiment 6. In this way, in spite of density change, the same AVP distribution is observed. Longer residence time of experiment 7 explains the difference in oligomers with experiment 6. The distribution of the AVP of experiment 6, is independent of the change in pKw, as was discussed above for experiments 4 and 6. The highest yield of glycolaldehyde-pyruvaldehyde (calculated as mass of product/mass of soluble material in raw biomass) was obtained for experiment 7 (24.4%), probably due to the combination of higher H+ concentration and longer *t*.

A different AVP distribution is observed in the experiment 9, where lactic acid is the most abundant product and acetic acid is depleted compared to the experiment 4 and 6 (see Fig. 2 (d)). This finding could be explained by the short *t* of the mixture at high temperature, conditions in which the reactions are stopped after lactic acid production in the retro-aldol route, inhibiting the acetic acid formation. This selectivity seems to take place in the SHR mainly during the first stage of temperature in the reactor R.1. After that, the formation of lactic acid in the SHR is reduced. The highest yield of lactic acid was found at Experiment 9 (25.5%). The water flow increase in the first reactor has no clear effect on the production of retro-aldol compounds (see reactions 10 and 11 in Fig. 2 (d)). Under these conditions, the oligomers breakup seems to become slower, since their amount is enlarged related to the monomeric sugars. In both cases, the retro aldol pathways are followed producing glycolaldehyde-pyruvaldehyde and lactic acid with similar yields.

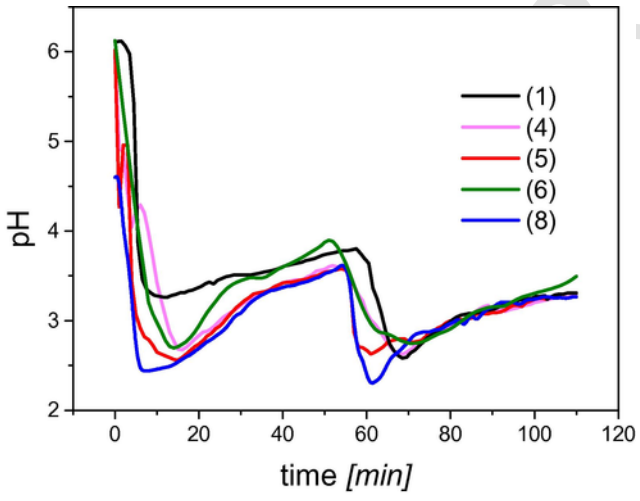

Fig. 4. pH of the liquid product vs time. Comparison of the reactions at low (experiments 4 and 6) and high conversions (experiments 5 and 8) at sub and supercritical conditions of water.

The combination of many variables influencing the distribution of a large number of products, involved in a complex reaction path as the described in Fig. 3, is hard to be easily explained. Furthermore, as was mentioned above, we are dealing with the hydrolysis of a real biomass, in which other components could be influencing the observed behavior.

3.3. Hydrolysis kinetic model

Aiming to analyze further the results obtained by the coupled system, a kinetic model for the second reactor is proposed in this section. This model takes into account the solubilized biomass composition fed to the second reactor. It was specially focused on the time period corresponding to the first stage of the solubilization (at the conditions of experiment 1) since this step produces an outlet stream with higher amount of the chemicals of interest (see last two columns of Table 1). The bigger added valued compounds production from stage 1 is due to the fact that the operational temperature was around 180 °C, which means a lower degradation. The reaction pathway proposed in this caseis showed in Fig. 5. It is a simplified version of the real hydrolysis described in Fig. 3. The modelling was done by the transient regime mass balances for each compound in the fluid: oligomers, sugars and products (Eq. (3)). Moreover, the following assumptions have been considered: (1) the reaction order for all the kinetics is 1 for the biomass compound and proton concentration in water, (2) there are no diffusional effects in fluid phase, (3) kinetic constants follows Arrhenius' law and (4) the reactor works at the same temperature at any point. Regarding kinetics, a conventional expression was used including the effect of the concentration of water proton since it is a hydrolysis process (Eq. (4)).

$$\frac{\delta C_{L_j}}{\delta t} = r_j - \frac{u}{L}\cdot\frac{\delta C_{L_j}}{\delta z} \tag{3}$$

$$r_j = C_{H^+}\cdot\sum_{i=1}^{i=N}\propto_{i,j}\cdot K_{L_i}\cdot C_{L_i} \tag{4}$$

3.3.1. Numerical resolution

Eq. (3) is a set of 6 partial differential equations (PDE) which has to be discretized to obtain a set of ordinary differential equation (ODE). The resolution of this set of ODEs was performed by the Runge-Kutta's method with a 8th convergence order and the discretization by coupling orthogonal colocation method on finite elements [46]. The fitting of the experimental data constitutes an optimization problem. Due to its complexity, it was previously seeded by

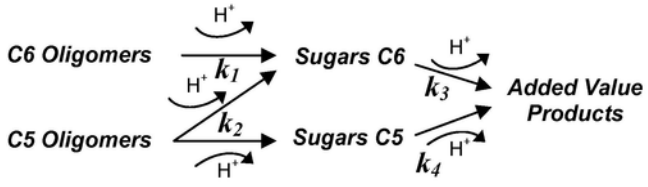

Fig. 5. Simplified reaction pathway for solved biomass hydrolysis.

manual iteration, and then, optimized by the Nelder-Mead-Simplex method. Moreover, as the inlet concentration of the hydrolysis reactor was variable and the oligomer properties changed with extraction time [47], the problem was optimized at every experimental point. Finally, the solution was reviewed in order to ensure the physical meaning of the parameters. The objective function was the minimization of the Absolute Average Deviation (A.A.D., Eq. (5)) for oligomer, sugar and products concentration at the SHR output.

$$A.A.D. = \sum_{i=1}^{n} \frac{1}{n} \cdot \left| \frac{X_{\exp} - X_{sim}}{X_{\exp}} \right| \cdot 100 \quad (5)$$

3.3.2. Experimental data fittings

In order to validate the model, only experiments 4, 6 and 9 were used because they were carried out at similar residence times and three different temperatures (see Table 1). For experiment 4, the data at extraction time of 9 and 14 min were not considered because they do not follow the tendency fixed by the set of the three experiments used (4, 6 and 9). Moreover, as each experiment was carried out independently, the inlet for the reactor was assumed to have the same composition that experiment 1 but with TOC profile of the fitted experiment (4, 6 and 9). It is also remarkable that the volumetric flow was the addition of the provided flow by the two pumps for all the experiments (see Fig. 1). The deviation between the model and the experimental data is arrayed in Table 2 and for experiment 6 it also can be seen in Fig. 6. The model was able to reproduce successfully the hydrolysis of solubilized biomass, being the average A.A.D. 21.14%, 37.37%, 18.41% and 7.24% for instant hemicellulose and cellulose oligomers, sugars C6, sugars C5 and their degradation products (the added value products respectively or AVP). These discrepancies changed to 27.46%, 7.61%, 9.31% and 3.99% respectively when cumulated values were used. Taking into account these last values, it can be checked that the highest error is in the estimation of the oligomers mass, which can be caused by the fact that the experimental data were obtained by the difference between the TOC and the sum of the other compounds (sugars and AVP). Moreover, the deviation between the experimental and simulated TOC was also calculated in order to check that the mass conservation law is followed. For all the cases, this mass balance deviation result in zero percent with three significant figures (0.00%). The kinetic constants and the stoichiometric coefficients (K_{L_i} and $\propto_{i,j}$ in Eq. (4), respectively) had

Table 2
Average absolute deviation of the fittings (experiments 4, 6 and 9) and simulations (experiments 5 and 8).

Experiment	ADD %							
	Instantaneous				Cumulated			
	Oligomers[1]	C6[2]	C5[3]	AVP[4]	Olig[1]	C6[2]	C5[3]	AVP[4]
4	21.70	21.88	21.92	7.38	26.85	10.78	4.98	7.52
6	20.58	29.11	22.16	6.27	6.99	2.15	14.82	1.78
9	*	61.04	11.15	8.07	48.53	9.90	8.15	2.66
Average	21.14	37.34	18.41	7.24	27.46	7.61	9.31	3.99
5	*	*	*	5.77	*	*	*	4.94
8	*	*	*	0.93	*	*	*	1.02
Average	*	*	*	4.65	*	*	*	3.32

[1] Oligomers from hemicellulose and cellulose.
[2] Sugars C6.
[3] Sugars C5.
[4] Degradation products.
* Compound not detected. ADD % of total organic content was 0.0.

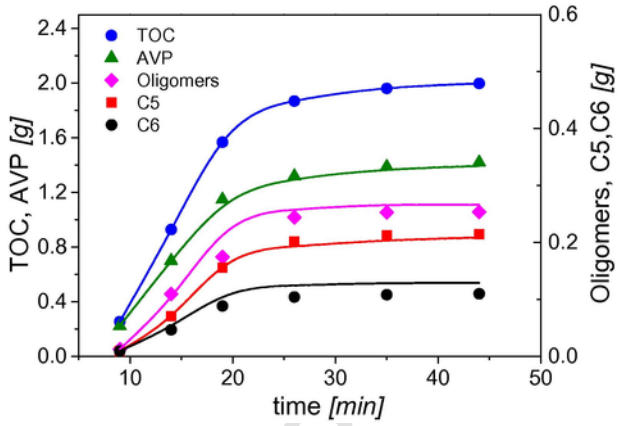

Fig. 6. Experimental and simulated amounts of soluble material by TOC, C5 + C6 Oligomers, sugars C6, sugars C5 and added value products obtained in experiment 6. Symbols represents the experimental values and continuous lines represents the results of the kinetic model using the optimized kinetic parameters.

to be obtained from fitting. Regarding $\propto_{i,j}$, it was always 1 less for the final products coming from hemicellulose oligomers since they are composed by pentoses and hexoses [48,49]. These fitted parameters, which are shown in Table 4, require a deeper analysis and they are discussed in the next section.

3.3.3. Analysis of kinetic parameters

The dependence of the kinetics parameters with temperature was proved. The regression coefficient (R^2) according the Arrhenius' theory was higher than 0.84 for all the cases (see Table 3). No change in the kinetic behavior was observed through the critical point (see Table 3) like does in the hydrolysis of microcrystalline cellulose [44,50] according to the commented in Section 3.2.2, since there is not simultaneous solubilization in the SHR. However, a dependence of the kinetic behavior was observed with the extraction time, since the rates of production of valuable chemicals is decreased after the maximum of solubilized mass is reached (see Fig. 7 (a) and (b)). This observation could be related with the influence of some of the chemicals produced by the further hydrolysis of sugars on the hydrothermal hydrolysis. In addition, it is also interesting that after this change, the kinetics of the sugar transformation tend to their initial value while the kinetic of the oligomer breakdown grows exponentially. This difference would be originated by the changes in the molecular weight of the extracted oligomers and the fact that they would be transformed more quickly if the molecular weight is lower. Moreover, it

Table 3
Regression coefficient (R^2) of the Activation Energy with temperature for the kinetic constants showed in Fig. 5.

t_e[1][min]	k_1[a]	k_2[b]	k_3[c]	k_4[d]
	R^2			
19	0.88	0.87	0.99	0.999
26	0.88	0.86	0.99	0.98
35	0.87	0.85	0.99	0.97
44	0.93	0.89	0.9999	0.96
Average	0.89	0.87	0.99	0.97

[a] Cellulose oligomer cleavage constant.
[b] Hemicellulose oligomer cleavage constant.
[c] Sugars C6 hydrolysis kinetic constant.
[d] Sugars C5 hydrolysis kinetic constant.
[1] Fractionation time.

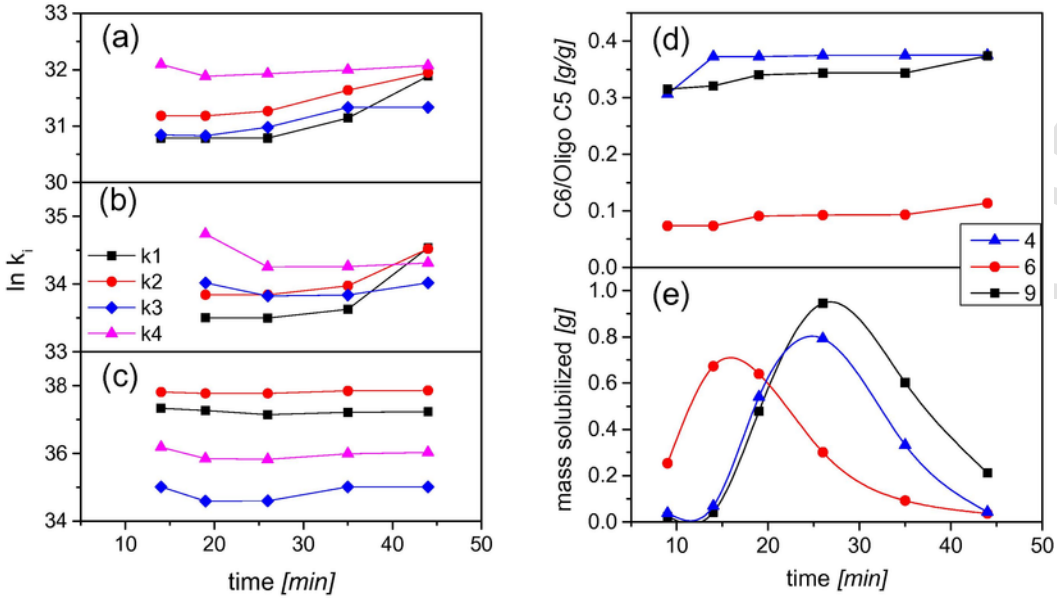

Fig. 7. Evolution of the logarithm of the kinetic constants for experiment 6(a), 4(b) and 9 (c). Ratio C6/OligoC5 (d). Solubilized mass with the extraction time for the experiments 6, 4 and 9 (e). k_1: Cellulose oligomer breakup kinetic constant, k_2: Hemicellulose oligomer breakup kinetic constant, k_3: Sugars C6 hydrolysis kinetic constant, k_4: Sugars C5 hydrolysis kinetic constant.

can be seen that temperature can compensate this negative effect, being negligible for oligomers at 400 °C (Fig. 7 (c)).

Other interesting result is the evolution of the ratio between the four kinetic constants. In Section 3.2.1 it was indicated that sugar transformation is faster than oligomer cleavage in subcritical conditions and lower in supercritical water. This behavior agrees with the obtained from the fittings, but only before the time of maximum of extraction (Fig. 7 (a) and (c)). So, from this point, the changes in molecular weight and the raw material transformation makes the oligomer cleavage always greater. As the oligomer composition changes with extraction time, the kinetic cannot be reproduced by a typical Arrhenius' kinetic. So, two equations function of this time (t_e) are proposed, one for the oligomer cleaving (Eq. (6)) and other for the sugar further reactions (Eq. (7)).

$$CKP = C \cdot \left| t_{e_{max}} - A \cdot t_e \right|^B \quad (6)$$

$$CKP = D + \frac{E}{1 + e^{(F \cdot (t_e - G))}} \quad (7)$$

where CKP refers to both, the activation energy (Ea/R) and the natural logarithm of the pre-exponential factor (ln(k)). In Eq. (6), the parameter *C* is the natural logarithm of the pre exponential factor or activation energy at the maximum extraction time ($t_{e_{max}}$) and parameters *A* and *B* introduce the effect of the changes in the structure and reaction medium. A would be related with the strong of the compound against its degradation by hydrolysis. B would be a measure of how structure or reaction medium can accelerate or restrain the degradation. In Eq. (7), *D* is the pre exponential factor or the activation energy at the time where the biggest solubilization takes place, *E* and *F*, are the parameters that consider the role of the structure and reaction medium and *G* is the time when the maximum extraction is reached. In this case, E would represent how the medium or the structure can enhance the hydrolysis or hinder it. F would be the compound resistance against degradation.

Finally, the evolution of the hexoses content in hemicellulose oligomers is represented in Fig. 7 (b). It can be observed that the ratio between these values grows with time. This result was expected because hexoses would make the dissolution more difficult and would explain the fact that in experiment 5 the extraction was faster than 4 and 9 experiments (see Fig. 7 (c)). Moreover this result agrees with the data reported by other authors [51].

3.3.4. Simulated experiments

As it was mentioned in Section 3.3.2, only experiments 4, 6 and 9 were used to validate the model. Experiments 5 and 8 were not considered because their reaction time were much higher, which implies almost a total conversion at the reactor outlet. However, it was checked if the model was able to reproduce their behavior. The result of the simulations are presented in Fig. 8, being the absolute devia-

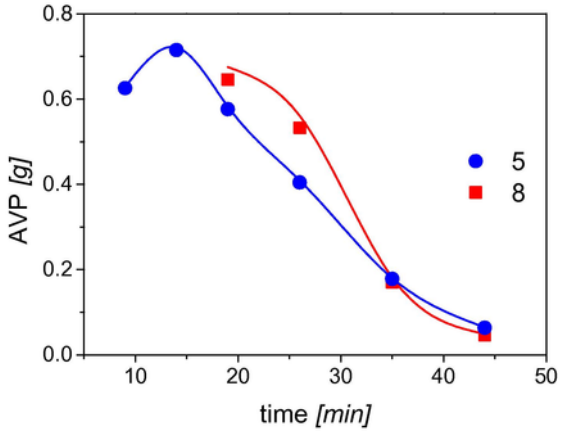

Fig. 8. Comparison between the experimental and simulated data for AVP in experiment 5 and 8. Symbols are the experimental data and full lines shows the prediction of the model with optimized kinetic parameters for each data.

tion around 4% for both experiments. Therefore, the model can predict successfully the hydrolysis at both low (0.2–1.0 s) and high (11.1–12.5 s) residence times.

3.3.5. Model limitations

From the results showed in the three previous sections, the model was able to successfully reproduce the experimental behavior of the set-up. In fact, this model can be used for any other lignocellulosic biomass because of the fact that it has been developed for a general biomass hydrolysis pathway. However, it is limited to processes where soluble lignin is low and when the aim is to reproduce the overall behavior of a solubilized biomass stream hydrolysis instead of an analysis of each individual compound. Furthermore, this model can be also adapted to processes where the inlet stream is variable in time.

4. Conclusions

A new process coupling fractionation and hydrolysis steps was developed. By means of this process, up to 64.2% of feed Holm oak wood was solubilized mainly as oligomers of hexoses and pentoses and sugars with a small fraction of retro-aldol compounds. The low ratio of the amount of oligomers to monomeric sugars in the outlet stream could be explained by a similar behavior than in the case of pure cellulose hydrolysis: the rate of monomers hydrolysis is higher to the oligomers break up in subcritical conditions, but this tendency is reverted at supercritical temperatures.

The main products of the further hydrolysis in the second reactor were glycolaldehyde, pyruvaldehyde and lactic acid. Yield (related to the amount of soluble sugars in the raw biomass) of 24 wt% of Glycolaldehyde-Pyruvaldehyde was found at long reaction times (350 °C, 160 bar and 8.6 s) and 25 wt% of lactic acid was found at short reaction time but high temperature (400 °C, 250 bar and 0.23 s). An increasing amount of acetic acid was observed at the highest residence times (e.g. 12 s).

The distribution of products is related to a combined reaction hydrolysis pathway of cellulose and hemicellulose involving oligomer cleavage to monomers, isomerization steps and two competing paths: retro-aldol condensation and dehydration. The influence of the water density and the amount of ions H^+ coming from the dissociation process is not clear as it is in the case of the hydrolysis of pure cellulose, in which the glucose dehydration is highly inhibited and retro aldol pathways clearly favored at temperatures and pressures above the water critical point. In the present work, products coming from retro-aldol paths as well as products of dehydration are observed in both conditions: sub and supercritical. Finally, a general kinetic modelling for the hydrolysis reactor was proposed. This model could reproduce the experimental data for sugar and added value products with deviations lower than 10%. Besides, the calculated kinetic parameters reproduced the changes in oligomer and sugar conversion when the hydrolysis is performed in supercritical conditions instead of in subcritical water. This model can be applied to any other lignocellulosic biomass with a low content of soluble lignin.

The main advantage of this combined process consist in providing a liquefied biomass stream to a selective hydrolysis reactor giving the valorization of the raw material avoiding the costly grinding of particles from several millimeters to less than two hundred microns needed to pump it in a water stream belonging to a high pressure process.

Acknowledgements

The authors acknowledge the Spanish "Ministerio de Economía y Competitividad (MINECO)" and FEDER funds, Project BioFraHynery CTQ2015-64892-R and the regional government (Junta de Castilla y León), Project Reference: VA330U13 for funding. MEng. Gianluca Gallina wishes to acknowledge the Spanish "Ministerio de Economía y Competitividad (MINECO)" for the scholarship/predoctoral contract BES-2013-063556. MEng. Alvaro Cabeza would like to thank to the Spanish "Ministerio de Educación, Cultura y Deporte", training program of university professors (reference FPU2013/01516) for the research training contract.

Appendix A. Supplementary data

Supplementary data associated with this article can be found, in the online version, at http://dx.doi.org/10.1016/j.cej.2016.09.007.

Table 4
Fitted parameters used to estimate the kinetic constants depending on the extraction time.

k_1[a]	ln(k)[e]	Ea/R[f]	k_2[b]	ln(k)[e]	Ea/R[f]
	–	[K]		–	[K]
A	1.04	1.03	A	1.08	1.08
B	0.04	0.06	B	0.03	0.05
C	106	46,543	C	109	48,553
k_3[c]	ln(k)[e]	Ea/R[f]	k_4[d]	ln(k)[e]	Ea/R[f]
	–	[K]		–	[K]
A	3.26	2069	A	2.85	1834
B	22.05	24.22	B	21.25	20.15
C	1.35	4.01	C	1.70	3.58
D	87.32	35,238	D	89.63	36,081

[a] Cellulose oligomer breakup constant.

[b] Hemicellulose oligomer breakup constant.

[c] Sugars C6 hydrolysis constant.

[d] Sugars C5 hydrolysis constant.

[e] Natural logarithm of the Arrhenius' pre-exponential factor.

[f] Activation energy.

References

[1] N. Akiya, P.E. Savage, Roles of water for chemical reactions in high-temperature water, Chem. Rev. 102 (2002) 2725–2750.

[2] P.E. Savage, S. Gopalan, T.I. Mizan, C.J. Martino, E.E. Brock, Reactions at supercritical conditions: applications and fundamentals, AIChE J. 41 (1995) 1723–1778.

[3] D.A. Cantero, M.D. Bermejo, M.J. Cocero, Reaction engineering for process intensification of supercritical water biomass refining, J. Supercrit. Fluids (2014) http://dx.doi.org/10.1016/j.supflu.2014.1007.1003.

[4] A.J. Ragauskas, C.K. Williams, B.H. Davison, G. Britovsek, J. Cairney, C.A. Eckert, W.J. Frederick, J.P. Hallett, D.J. Leak, C.L. Liotta, J.R. Mielenz, R. Murphy, R. Templer, T. Tschaplinski, The path forward for biofuels and biomaterials, Science 311 (2006) 484–489.

[5] A.A. Peterson, F. Vogel, R.P. Lachance, M. Fröling, J.M.J. Antal, J.W. Tester, Thermochemical biofuel production in hydrothermal media: a review of sub- and supercritical water technologies, Energy Environ. Sci. 1 (2008) 32.

[6] D.A. Cantero, C. Martinez, M.D. Bermejo, M.J. Cocero, Simultaneous and selective recovery of cellulose and hemicellulose fractions from wheat bran by supercritical water hydrolysis, Green Chem. (2015) http://dx.doi.org/10.1039/c4gc01359j.

[7] P. Gullón, A. Romaní, C. Vila, G. Garrote, J.C. Parajó, Potential of hydrothermal treatments in lignocellulose biorefineries, Biofuels, Bioprod. Biorefin. 6 (2012) 219–232.

[8] T.H. Kim, Y.Y. Lee, Fractionation of corn stover by hot-water and aqueous ammonia treatment, Bioresour. Technol. 97 (2006) 224–232.

[9] M. Sasaki, T. Adschiri, K. Arai, Fractionation of sugarcane bagasse by hydrothermal treatment, Bioresour. Technol. 86 (2003) 301–304.

[10] M. Sasaki, T. Adschiri, K. Arai, Kinetics of cellulose conversion at 25 MPa in sub- and supercritical water, AIChE J. 50 (2004) 192–202.

[11] D.A. Cantero, M. Dolores Bermejo, M. José Cocero, High glucose selectivity in pressurized water hydrolysis of cellulose using ultra-fast reactors, Bioresour. Technol. 135 (2013) 697–703.

[12] Z. Fang, C. Fang, Complete dissolution and hydrolysis of wood in hot water, AIChE J. 54 (2008) 2751–2758.

[13] H.R. Holgate, J.C. Meyer, J.W. Tester, Glucose hydrolysis and oxidation in supercritical water, AIChE J. 41 (1995) 637–648.

[14] Y. Chen, Y. Wu, R. Ding, P. Zhang, J. Liu, M. Yang, P. Zhang, Catalytic hydrothermal liquefaction of D. tertiolecta for the production of bio-oil over different acid/base catalysts, AIChE J. 61 (2015) 1118–1128.

[15] Y. Wang, F. Jin, M. Sasaki, F. Wahyudiono, Z. Wang, M..Goto. Jing, Selective conversion of glucose into lactic acid and acetic acid with copper oxide under hydrothermal conditions, AIChE J. 59 (2013) 2096–2104.

[16] X. Yan, F. Jin, K. Tohji, A. Kishita, H. Enomoto, Hydrothermal conversion of carbohydrate biomass to lactic acid, AIChE J. 56 (2010) 2727–2733.

[17] O. Bobleter, Hydrothermal degradation of polymers derived from plants, Prog. Polym. Sci. 19 (1994) 797–841.

[18] M. Sasaki, K. Goto, K. Tajima, T. Adschiri, K. Arai, Rapid and selective retro-aldol condensation of glucose to glycolaldehyde in supercritical water, Green Chem. 4 (2002) 285–287.

[19] B.M. Kabyemela, T. Adschiri, R. Malaluan, K. Arai, Degradation kinetics of dihydroxyacetone and glyceraldehyde in subcritical and supercritical water, Ind. Eng. Chem. Res. 36 (1997) 2025–2030.

[20] B.M. Kabyemela, T. Adschiri, R.M. Malaluan, K. Arai, Glucose and fructose decomposition in subcritical and supercritical water: detailed reaction pathway, mechanisms, and kinetics, Ind. Eng. Chem. Res. 38 (1999) 2888–2895.

[21] B.M. Kabyemela, T. Adschiri, R.M. Malaluan, K. Arai, Kinetics of glucose epimerization and decomposition in subcritical and supercritical water, Ind. Eng. Chem. Res. 36 (1997) 1552–1558.

[22] X. Lü, S. Saka, New insights on monosaccharides' isomerization, dehydration and fragmentation in hot-compressed water, J. Supercrit. Fluids 61 (2012) 146–156.

[23] Y. Román-Leshkov, M. Moliner, J.A. Labinger, M.E. Davis, Mechanism of glucose isomerization using a solid lewis acid catalyst in water, Angew. Chem. Int. Ed. 49 (2010) 8954–8957.

[24] M. Bicker, S. Endres, L. Ott, H. Vogel, Catalytical conversion of carbohydrates in subcritical water: a new chemical process for lactic acid production, J. Mol. Catal. A: Chem. 239 (2005) 151–157.

[25] M. Bicker, D. Kaiser, L. Ott, H. Vogel, Dehydration of D-fructose to hydroxymethylfurfural in sub- and supercritical fluids, J. Supercrit. Fluids 36 (2005) 118–126.

[26] D.C. Elliott, P. Biller, A.B. Ross, A.J. Schmidt, S.B. Jones, Hydrothermal liquefaction of biomass: developments from batch to continuous process, Bioresour. Technol. 178 (2015) 147–156.

[27] W. Reynolds, H. Singer, S. Schug, I. Smirnova, Hydrothermal flow-through treatment of wheat-straw: detailed characterization of fixed-bed properties and axial dispersion, Chem. Eng. J. 281 (2015) 696–703.

[28] Y. Yu, H. Wu, Effect of ball milling on the hydrolysis of microcrystalline cellulose in hot-compressed water, AIChE J. 57 (2011) 793–800.

[29] Y. Zhao, S. Zhang, J. Chen, Mechanisms of sequential dissolution and hydrolysis for lignocellulosic waste using a multilevel hydrothermal process, Chem. Eng. J. 273 (2015) 37–45.

[30] M.J. González-Muñoz, S. Rivas, V. Santos, J.C. Parajó, Aqueous processing of Pinus pinaster wood: kinetics of polysaccharide breakdown, Chem. Eng. J. 231 (2013) 380–387.

[31] S. Kilambi, K.L. Kadam, Production of fermentable sugars and lignin from biomass using supercritical fluids, US Patent, Google Patents, United States of America, 2013.

[32] D.A. Cantero, M.D. Bermejo, M.J. Cocero, Kinetic analysis of cellulose depolymerization reactions in near critical water, J. Supercrit. Fluids 75 (2013) 48–57.

[33] A. Sluiter, B. Hames, R. Ruiz, C. Scarlata, J. Sluiter, D. Templeton, D. Crocker, Determination of Structural Carbohydrates and Lignin in Biomass, National Renewable Energy Laboratory, U.S. Department of Energy, Golden, Colorado, 2011.

[34] A. Sluiter, B. Hames, R. Ruiz, C. Scarlata, J. Sluiter, D. Templeton, Determination of Sugars, Byproducts, and Degradation Products in Liquid Fraction Process Samples, National Renewable Energy Laboratory, U.S. Department of Energy, Golden, Colorado, 2006.

[35] P. Mäki-Arvela, T. Salmi, B. Holmbom, S. Willför, D.Y. Murzin, Synthesis of sugars by hydrolysis of hemicelluloses – a review, Chem. Rev. 111 (2011) 5638–5666.

[36] X.-F.C.S.-N. Sun, H.-Y. Li, F. Xu, R.-C. Sun, Structural characterization of residual hemicelluloses from hydrothermal pretreated Eucalyptus fiber, Int. J. Biol. Macromol. 69 (2014) 158–164.

[37] R. Fletcher, A Modified Marquardt Subroutine for Nonlinear Least Squares, United Kingdom Atomic Energy Authority, Harwell, 1971.

[38] G. Gallina, Á. Cabeza, P. Biasi, J. García-Serna, Optimal conditions for hemicelluloses extraction from Eucalyptus globulus wood: hydrothermal treatment in a semi-continuous reactor, Fuel Process. Technol. 148 (2016) 350–360.

[39] B.A. Miller-Chou, J.L. Koenig, A review of polymer dissolution, Prog. Polym. Sci. 28 (2003) 1223–1270.

[40] Y. Zhao, W.J. Lu, H.T. Wang, Supercritical hydrolysis of cellulose for oligosaccharide production in combined technology, Chem. Eng. J. 150 (2009) 411–417.

[41] M. Sasaki, T. Hayakawa, K. Arai, T. Adschiri, Measurement of the rate of retro-aldol condensation of D-xylose in subcritical and supercritical water, in: W.S.P. Co. (Ed.) 7th International Symposium Hydrothermal Reactions Singapore, 2003, pp. 169–176.

[42] T.M. Aida, N. Shiraishi, M. Kubo, M. Watanabe, R.L. Smith Jr, Reaction kinetics of D-xylose in sub- and supercritical water, J. Supercrit. Fluids 55 (2010) 208–216.

[43] H. Kimura, M. Nakahara, N. Matubayasi, In situ kinetic study on hydrothermal transformation of D-glucose into 5-hydroxymethylfurfural through D-fructose with 13C NMR, J. Phys. Chem. A 115 (2011) 14013–14021.

[44] D.A. Cantero, Á. Sánchez Tapia, M.D. Bermejo, M.J. Cocero, Pressure and temperature effect on cellulose hydrolysis in pressurized water, Chem. Eng. J. 276 (2015) 145–154.

[45] W.L. Marshall, E.U. Franck, Ion product of water substance, 0–1000 °C, 1–10,000 bars New International Formulation and its background, J. Phys. Chem. Ref. Data 10 (1981) 295–304.

[46] W. Press, S. Teukolsky, W. Vetterling, B. Flannery, Numerical Recipes 3rd Edition: The Art of Scientific Computing, 2007.

[47] A. Cabeza, C.M. Piqueras, F. Sobrón, J. García-Serna, Modeling of biomass fractionation in a lab-scale biorefinery: Solubilization of hemicellulose and cellulose from holm oak wood using subcritical water, Bioresour. Technol. 200 (2016) 90–102.

[48] O. Bobleter, Hydrothermal degradation of polymers derived from plants, Prog. Polym. Sci. (Oxford) 19 (1994) 797–841.

[49] W.H.P. Harmsen, L. Bermudez, R. Bakker, Literature Review of Physical and Chemical Pretreatment Processes for Lignocellulosic Biomass, Wageningen UR Food & Biobased Research, 2010.

[50] M. Sasaki, B. Kabyemela, R. Malaluan, S. Hirose, N. Takeda, T. Adschiri, K. Arai, Cellulose hydrolysis in subcritical and supercritical water, J. Supercrit. Fluids 13 (1998) 261–268. http://www.sciencedirect.com/science/article/pii/S0896844698000606.

[51] S.-N. Sun, X.-F. Cao, H.-Y. Li, F. Xu, R.-C. Sun, Structural characterization of residual hemicelluloses from hydrothermal pretreated Eucalyptus fiber, Int. J. Biol. Macromol. 69 (2014) 158–164.